Randles Model of Vitreous Humor

Tjerignimin Silue, Saugandhika Minnikanti and Nathalia Peixoto
Electrical and Computer Engineering, George Mason University, Fairfax, VA, U.S.A.

Keywords: Vitreous Humor, Stainless Steel Electrodes, Electrochemistry, Characterization, Cyclic Voltammetry, Electrochemical Impedance Spectroscopy, Randles Model.

Abstract: The vitreous is a gel-like structure found in the eyes. It is located above the retina to prevent the passage of fluids. As aging occurs, the vitreous can liquefy and can cause retinal detachment. The literature has little characterization of the vitreous, as it is often a less interesting structure than the retinal tissue. We investigate the impedance properties of the stimulation electrodes such as the constant phase element (Q) and the resistance of the solution (R_{sol}). We show results on vitreous characterization through electrochemical methods as a first step toward understanding the role of electrical stimulation in retinal prosthetics applications as it pertains to vitreous liquefaction. Our objective is to characterize the vitreous for a wide frequency range and to determine how charge is distributed through its conductive structure. Our electrochemical experiments were performed using insulated stainless steel electrodes (1) in phosphate buffered saline (PBS) and (2) in thimerosal as controls, (3) in vitreous without thimerosal, as well as (4) in vitreous preserved with thimerosal. We also performed cyclic voltammetry to measure the cathodic charge storage capacity for the electrodes for all experimental groups. Our results showed that the resistivity of the vitreous increases as thimerosal is added and that the cathodic charge storage capacity of the vitreous does not show any significant difference in the means as thimerosal is added.

1 INTRODUCTION

Retinal prostheses for the blind are in clinical trials world-wide. Each retinal prosthesis attempts to position the stimulus electrode array in close proximity to the retina in order to effectively activate the remaining retina neural circuitry (Majdi et al., 2014). Stimulus pulses can be remarkably attenuated by resistive and capacitive barriers in the eye wall as well as the vitreous (Majdi et al., 2014), which in some cases could prevent effective activation of the retinal tissue. Poorly placed electrode arrays can lose charge through this gel like conductive structure called the vitreous humor.

The vitreous humor is a virtually acellular, jelly adhesive-like, highly hydrated extracellular substance located above the retina to prevent rapid passage of fluid into holes which may exist in the retina (Joseph, 1990). A network of thin unbranched collagen fibrils that are mixed in composition, comprising collagen types II, V/XI and IX, maintains the gel-like structure in a rabbit model (Bishop, 2000). The vitreous humor contains two chemically specific proteins: mucoid and vitrein. The mucoid fills the gap of the micelles of the vitrein, which prevents it from diffusing away. The chemical distribution of the vitrein in the vitreous humor suggests that the vitreous humor is not strictly a uniform gel and that the vitreous membrane is composed of vitrein (Krause, 1934).

During ageing, the gel can liquefy. In about 30% (Bishop, 2000) of the population, the residual gel structure eventually collapses away from the posterior retina in a process called vitreous detachment. This process plays an important role in a number of common blinding conditions including rhegmatogenous retinal detachment, proliferative diabetic retinopathy and macular hole formation (Bishop, 2000). Thus, understanding molecular events underlying vitreous liquefaction and vitreous detachment may lead to new retinal prostheses to improve retina degenerative diseases caused by vitreous detachment.

Retinal prostheses are implants with custom circuits that electrically stimulate retinal cells through electrodes. Recent results point to confounding variables that might have been overlooked as significant in earlier designs such as the influence of the vitreous humor (Shah et al., 2007). For example, sticking of the vitreous to the

Silue T., Minnikanti S. and Peixoto N.
Randles Model of Vitreous Humor.
DOI: 10.5220/0006166001560162
In *Proceedings of the 10th International Joint Conference on Biomedical Engineering Systems and Technologies (BIOSTEC 2017)*, pages 156-162
ISBN: 978-989-758-216-5

retina may change the impedance seen by the electrodes when they are positioned at the surface of the retina. Recent studies examined the electrical properties of the retinal-electrode interface and showed that the tissue resistance of the retina is greater than that of the vitreous humor in the eye but little is known about the electrical behavior of the vitreous humor (Shah et al., 2007). In order to perform experiments of reasonable length in any biological tissue, traditionally the tissue is kept in media. For vitreous humor, previous research has demonstrated that the use of a preservative does not impact viscosity or other morphological characteristics of the sample (Kawano et al, 1982). Thimerosal is a methiolate sodium used in vaccines. In retinal research, thimerosal in a concentration of 0.005% is added in a small quantity (1 µl) to the vitreous for long-term observations. The addition of thimerosal at this concentration does not affect the viscosity of the vitreous (Kawano et al., 1982) which will be shown through vitreous characterization using electrochemical methods as a first step toward understanding its role during electrical stimulation in retinal prosthetics applications.

The objective is to investigate methods to reliably determine the characteristics of the vitreous from a stimulation electrode to the sample tissue extracted from rabbit eyes. As previously stated, characterizing the vitreous will aid in the determination of the conductivity of the structure, the location of the electrode within the eye, during the implant period. Both of these variables are critical for the long term success of implants. Currently available technology will be used and we hypothesized that, by measuring and analyzing impedance and charge delivery, we can establish the electrochemical characterization of the vitreous humor.

We will investigate how the impedance properties of the stimulation electrodes. In order to determine which factors influence the impedance, experimental data will be fitted to a Randles model and evaluated from the physical characteristics perspective. Solution resistance, charge transfer resistance, and constant phase elements, when taken together, determine the interface between the electrode and the electrolyte. The model can, in the future, be scaled to determine impedance models of the human eye can be used to demonstrate the effects of stimulation waveforms on the tissue.

In this study, we measured the electrical properties of the vitreous of the rabbit eye with implantable electrodes. We studied the electrochemical impedance spectroscopy of stainless steel electrodes of 250 µm diameter, insulated with Teflon (10 µm). We tested the impedance of the electrodes in four different scenarios: (1) in phosphate buffered saline (PBS), (2) in thimerosal (an organomercury compound), (3) in vitreous without thimerosal; as well as (4) in vitreous with thimerosal. We also performed cyclic voltammetry and measured the cathodic charge storage capacity for the electrodes for all experimental groups. Several electrical equivalent models were tested and fitted to the data to describe the physical system and provide insight into the actual model for the vitreous. We hypothesized that vitreous with and without thimerosal would therefore not change its electrical characteristics, given the low concentration of the preservative.

2 METHODS

Here we describe the utilized substrates and the electrochemical methods that were applied in order to characterize the vitreous samples.

2.1 Preparation of Vitreous and Solutions

A 1 ml of vitreous humor, stored in a 2 ml vial, was bought from a biological supply company (BioChemed Services, Winchester, VA). Thimerosal was acquired from Sigma-Aldrich (St. Louis, MO). A 0.005% of thimerosal solution was prepared with 5 mg of thimerosal ($C_9H_9HgNaO_2S$) dissolved in 100 ml of distilled water. 1 µl of the prepared 0.005% thimerosal solution was added to the extracted vitreous for preservation according to Kawano et al (Kawano et al., 1982). The final concentration of thimerosal in vitreous humor is $5x10^{-5}$ mg/ml.

2.2 Electrochemical Measurements

We manufactured clinically relevant stainless steel electrodes of 250 µm core-diameter, insulated with Teflon (10 µm) and characterized their electrochemical behavior in phosphate buffered saline, thimerosal and in vitreous. The electrode is micromanipulated and positioned in the vitreous sample, and electrochemical measurements were simultaneously taken. We recorded electrochemical impedance spectroscopy (EIS) and cyclic voltammetry (CV).

A high efficiency, research-grade potentionstat designed for fast and low-current measurements

(Reference 600+, Gamry, Warminster, PA) was used to perform measurements for the electrochemical characterization of the vitreous humor. Electrochemical Impedance Spectroscopy (EIS) and Cyclic Voltammetry (CV) was performed. To achieve EIS, a frequency response analyzer (FRA) is used to impose an AC signal to a cell. The AC voltage and current response of the cell is analysed by the FRA to determine the resistive, capacitive and inductive behaviour - the impedance - of the cell at that particular frequency (Loveday et al., 2001). On the other hand, CV is achieved by cycling potential to measure current. Characterization of the vitreous humor as well as the stainless steel electrode was performed in Phosphate Buffer Saline (PBS) and in the 0.005% thimerosal solution. The stainless steel electrodes were scanned from 1 Hz to 100 kHz for the EIS measurements and the CV curves were ran for 5 cycles at a scan rate of 100 mV/s. In addition, impedance spectra and CV of the stainless steel electrodes were performed in thimerosal diluted (0.005 %) in PBS and water. This was undertaken to investigate the properties of thimerosal and its effect on the electrodes.

For the purpose of our experiment, a two electrode setup was employed to measure the potential across the cell where the counter and reference terminals of the potentiostat were shorted and connected to an Ag/AgCl wire. The working and working sense were connected to a stainless steel wire electrode (250 µm in diameter, n = 5) for EIS and CV measurements of the vitreous humor (figure 1).

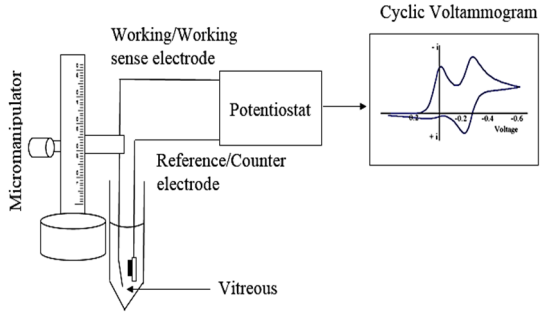

Figure 1: Schematic of experimental setup.

2.3 Data Analysis

The electrode is modelled by a Randles circuit, shown in figure 2, containing a constant phase element, indicated by (Q), and modelled as a non-linear capacitor which maintains the phase difference between current and voltage constant throughout the frequency spectrum. The constant phase element is parallel to a resistor (R_{ct}), and these two elements are commonly called pseudo-capacitance or polarization impedance in electrodes. The solution resistance of the vitreous, which is mainly water, is denoted by R_{sol}. The Randles circuit was generated for measuring the impedance between the electrode and ground, we applied a small (10 mVrms) sinusoidal wave of varying frequency, and measure the current through the circuit, that is, between the electrode and the Ag/AgCl wire. Reference and counter electrodes are shorted, given the low currents involved. The modulus of the measured impedance is then the amplitude difference between the applied voltage and measured current, and the phase angle of the impedance is the phase difference of both sinusoidal waves. By applying this method from 1 Hz to 100 kHz one obtains Nyquist and Bode plots (modulus and phase) of the combined impedance of the whole system: electrode, insulation, solution resistance.

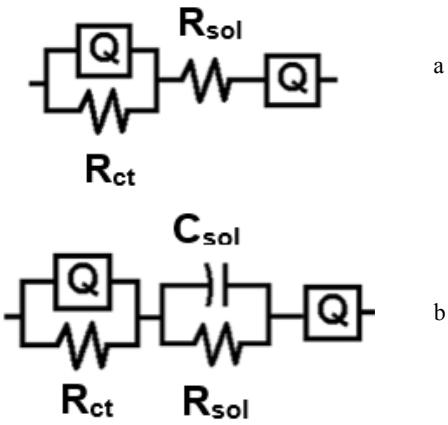

Figure 2a: Equivalent circuit model for PBS, vitreous, vitreous w/ thimerosal (distilled water) and thimerosal w/ PBS.
Figure 2b: Equivalent circuit model for thimerosal w/ distilled water.

ZSimpWin (EChem Software, Ann Arbor, MI) was used to develop the Randles circuit model (figure 2) from the EIS data. ZSimpWin employs the down-hill simplex method for optimizing the fits. Data were exported as text files from the Echem Analyst software (Gamry Instruments, Warminster, PA). The models presented with visual fit to Bode, Nyquist, real, and imaginary impedance values versus frequency plots, chi-squared value (χ^2) < 10×10^{-4}, relative standard errors < 15% and non-trending residual plots. As a two- electrode set up was employed, the measured EIS data will reflect

the properties of the working electrode (WE), of the media, and of the reference electrode (RE). Initially, impedance spectra obtained from PBS was fit to the model. The electrodes were modelled as a parallel connection of a constant phase element (Q) and the charge transfer resistance (R_{ct}). The reference and working electrodes were connected via a series resistance (R_{sol}) representing the media. The constant phase element arises due to surface non-uniformity and roughness of the interface. The impedance of the constant phase element is given by $Z = Yo\ (i\omega)\alpha$, where (Yo)-1 is a constant with dimension Fcm-2s(α-1), ω is angular frequency (2πf), $i = \sqrt{-1}$, and $0 < \alpha < 1$, where $\alpha = 1$ for an ideal capacitor. The results were obtained by averaging results from five electrodes (n=5) in each experimental group.

The measurement of how much charge can be delivered to tissue, by any electrode, is the integral of current over time, as $dQ/dt = I$, where Q is the charge in Coulombs, t is the time in seconds, and I is the current in Amperes. When the CV excitation voltage is applied at a slow rate, the hysteresis observed (difference between the positive and negative cycles of the voltage) denotes how much charge can held by the electrode. The area under the CV curve, is the charge storage capacity of the electrode, and a common parameter reported in the literature is the cCSC, cathodic charge storage capacity. This parameter is relevant in implants used for tissue stimulation because it sets the maximum possible charge transfer by a given electrode material and its geometrical area. This will allow for the evaluation of how well that specific electrode is performing during the implant period. CV tests to our experimental data will be shown and charge transfer mechanisms in vitro (with the electrode immersed in vitreous) will be evaluated.

3 RESULTS

The interplay between the electrode surface chemistry and the charge transfer into the vitreous solution was examined in detail by using voltammetric techniques. The system was stimulated with a quasi-DC voltage that ranged from -0.8V to 0.7V, this could vary depending on the electrode size and type. As the voltage is varied slowly over time (at 100 mV/s), the current flowing through the two electrodes was measured and plotted. Stability was determined and reduction and oxidation peaks on the current waveforms were observed. The cyclic voltammetry (CV) spectrum gave insights when the

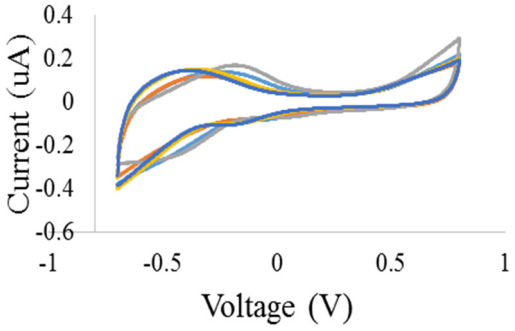

Figure 3: (Blue) thimerosal + PBS (0.005%), (Red) thimerosal + Distilled Water (0.005%), (Grey) PBS, (Orange) vitreous w/o thimerosal (0.005%), (Dark Blue) vitreous w/ Thimerosal (0.005%).

Table 1: Mean and standard deviation of the vitreous with and without thimerosal of all 5 electrodes. All values are in Coulombs (C).

	Vit+Thim	Vit-Thim
Mean	-1.63×10^{-6}	-1.46×10^{-6}
st. dev.	$\pm5.63\times10^{-7}$	$\pm2.35\times10^{-7}$

electrode was immersed in phosphate buffered saline, thimerosal versus when it is dipped into the vitreous.

The integration of the CV curve using EchemAnalyst provided the cathodic charge storage capacity (cCSC), expressed Coulombs (C), of the vitreous with thimerosal and the vitreous without thimerosal solutions (table 1). The mean cCSC was -1.63×10^{-6} C for vitreous with thimerosal and -1.46×10^{-6} C for vitreous without thimerosal while the standard deviation was $\pm5.63\times10^{-7}$ C for vitreous with thimerosal and $\pm2.35\times10^{-7}$ C for vitreous without thimerosal.

The mean and standard deviation of the charge storage capacity determined to characterize the electrode in vitreous with and without thimerosal provides information about the performance of the electrode in the electrolyte. Figure 3 shows the CV curves of the stainless steel electrode in the vitreous with and without thimerosal. A one-way ANOVA test was performed to determine the statistical significance of the means for each electrode. The p-value lower than 0.05 (p = 0.000, 0.012, 0.40, 0.008, 0.022 respectively) indicated that the mean difference between the vitreous with and without thimerosal is statistically different for all electrodes. A Tukey test was then performed to determine if there is a significant difference between the mean of the two groups. Results showed that the means are not significantly different. The insignificant

difference between the means is also observed in figure 3. The "vitreous w/o thimerosal" and "vitreous w/ thimerosal" voltammetric curves are similar, revealing that the charge transfer from the electrode to the vitreous is not significantly altered by the addition of thimerosal. If there had been any proteins adsorbed onto the surface of the electrode, then the "vitreous w/ thimerosal" spectrum would show significant differences to the "vitreous w/o thimerosal" spectrum.

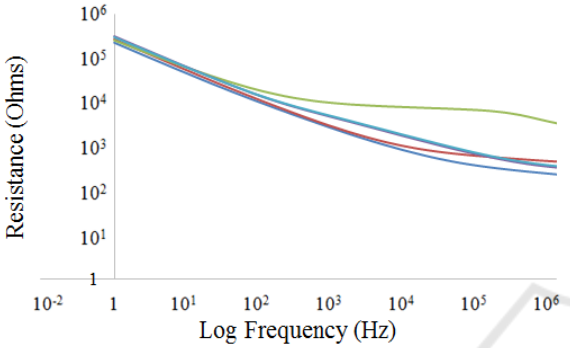

Figure 4A: Overlay of EIS impedance curves of a random electrode (Blue) thimerosal + PBS (0.005%), (Red) thimerosal + Distilled Water (0.005%), (Grey) PBS, (Orange) vitreous w/o thimerosal (0.005%), (Dark Blue) vitreous w/ thimerosal (0.005%).

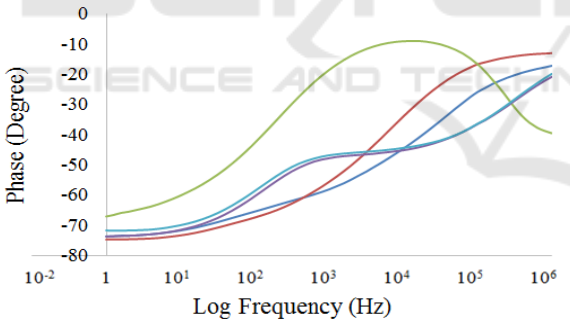

Figure 4B: Overlay of EIS phase curves of a random electrode (Blue) thimerosal + PBS (0.005%), (Red) thimerosal + Distilled Water (0.005%), (Grey) PBS, (Orange) vitreous w/o thimerosal (0.005%), (Dark Blue) vitreous w/ thimerosal (0.005%).

Table 2: Summary of the fitted parameter values with corresponding standard deviations to impedance spectra of stainless steel electrodes measured in PBS, vitreous and vitreous with 0.005% tthimerosal solution.

	PBS	Vitreous	Vitreous + thimerosal (0.005 % in dist. Water)
Q-Y_0-SS (uF)	6.49± 4.59	1.18 ± 1.28	1.59 ± 1.55
Q-n-SS	0.49± 0.13	0.54 ± 0.07	0.50 ± 0.07
R_{ct} (k Ω)	1.82 ± 1.15	24.49 ± 10.60	18.34 ± 8.56
R_{sol} (Ω)	473.55 ± 56.64	659.83 ± 310.60	1333.98 ± 1258.39
Q-Y_0-RE (uF)	0.12± 0.02	0.10 ±0.03	0.10 ± 0.03
Q-n-RE	0.85± 0.01	0.83 ± 0.02	0.83 ±0.02

Table 3: Summary of the fitted parameter values with corresponding standard deviations to impedance spectra of stainless steel electrodes measured in 0.005% thimerosal diluted in distilled water versus in PBS solutions.

	Thimerosal (0.005% in distilled water)	Thimerosal (0.005 % in PBS)
Q-Y_0-SS	60.40 ± 1.01 (nF)	6.84 ±3.28 (uF)
Q-n-SS	0.80 ± 0.10	0.43 ± 0.05
R_{ct} (kΩ)	65.36 ± 62.566	12.92 ± 18.31
C_{sol} (uF)	0.145 ± 0.04	N/A
R_{sol}	11.93 ± 5.54 GΩ	940.9±276.78 kΩ
Q-Y_0-RE	0.38 ± 0.22 (nF)	0.11 ± 0.03 (uF)
Q-n-RE	0.60 ± 0.07	0.85 ±0.01

Electrochemical impedance spectra of the electrodes were acquired for PBS, vitreous with and without thimerosal diluted with distilled water. Equivalent circuit model (figure 2) was fitted to the data (figure 4). The averaged parameters (n=5) are shown in table 2. The "solution" resistance (R_{sol}) is greater for vitreous in comparison to PBS. The estimated model parameters depict this trend (473.55 ± 56.64 Ω (PBS), 659.83 ± 310.60 Ω (vitreous)). The solution resistance further increases when thimerosal (0.005 %) is added to the vitreous (1.34 ± 1.25 kΩ). The RE electrode parameters are the same across all media. The constant phase element (Q) describes the deviation of the interfacial

impedance from the ideal behavior. The Q-n exponent values for the stainless steel electrode (SS) for PBS, vitreous and vitreous with thimerosal (0.005% in water) represent a deviation from a capacitive nature towards resistive (<0.6). The charge transfer occurring at the electrode-electrolyte interface is highest for vitreous and lowest in PBS while R_{ct} is lower when thimerosal is added to the vitreous. All the values are reported in the form of value ± standard deviation.

Impedance spectra were compared for thimerosal in distilled water versus PBS with the same dilution to understand its properties and effect on the electrodes performance. The averaged parameters (n=5) are shown in table 3. The "solution" resistance (R_{sol}) is not only greater when thimerosal (11.93 ± 5.54 GΩ) is diluted in water in comparison to PBS (940.90 ± 276.78 kΩ) but also presents a capacitive nature (0.145 ± 0.04 uF). Interestingly, the reference electrode parameters are different when the dilution media is changed (table 2). While the double layer capacitance is two orders of magnitude lower in the distilled water dilution (60.4 nF), versus PBS (6 µF), the Q-n exponent values for the stainless steel electrode (SS) is higher 0.80 ± 0.10, indicating the behaviour of a capacitor. As expected, the charge transfer resistance occurring at the electrode-electrolyte interface is higher for water dilution when comparing to PBS because the media is less conductive as expected. All the values are reported in the form of value ± standard deviation.

4 DISCUSSION

The effects of thimerosal diluted with PBS versus distilled water is determined with the "solution" resistance (R_{sol}). From our data, it is noticed that R_{sol} is only greater when thimerosal (11.93 ± 5.54 GΩ) is diluted in water in comparison to PBS (940.90 ± 276.78 k**Ω**) indicating its capacitive nature. This may be attributed to the low amount of free ions in distilled water in comparison to PBS. Moreover, the double layer capacitance lower in the distilled water dilution (60.40 ± 1.01 nF) with the higher Q-n exponent values (0.80 ± 0.10Ω) persists to conclude that thimerosal diluted with water has a capacitive behavior.

Though the RE electrode parameters is the same across all media, the "solution" resistance (R_{sol}) increases further when thimerosal (0.005 %) is added to the vitreous (1.34 ± 1.25 kΩ). This is true due to thimerosal containing ethylmercury, a compound that acts as both a substrate and an inducer (Clark et al., 1977). This property affects to the resistivity of the vitreous. This also explains why the Q-n exponent values for vitreous with thimerosal (0.005% in distilled water) deviated from capacitive nature towards resistive (<0.6) due to the added thimerosal.

The difference in the charge storage capacity of the vitreous with and without thimerosal shows that the ability of the electrode to deliver charge to the solution increases when dipped in the vitreous with thimerosal (table 1). The "solution" resistance reveals high conductivity for the vitreous solution w/o thimerosal versus the vitreous solution w/ thimerosal. The addition of the thimerosal solution w/ distilled water to the vitreous increased the mixture's resistivity while decreasing its electrical conductivity because of the resistance (11.93 ± 5.54 GΩ) of thimerosal diluted with distilled water.

5 CONCLUSION

The determined electrical properties of the vitreous with and without an organomercury compound with implantable electrodes allowed for a more detailed electrical representation of the vitreous. In retinal prostheses, the issue of the vitreous sticking to the retina presents itself. Since the resistivity of the vitreous increases when the thimerosal is added, it is expected to notice an increase in the impedance seen by the electrodes when they are positioned at the surface of the retina. Though the charge storage capacity is not significantly different as thimerosal is added, its addition leads to the increase of the solution resistance. This in turn decreases the electrical conductivity of the vitreous solution with thimerosal.

Our randles model and findings can be used to provide a starting point to assist regulators in understanding safety and effectiveness issues with the vitreous. It can also assist the retinal implant industry and device evaluators by establishing common metrics of device effectiveness and aid in a better understanding of the design issues that cause loss of effectiveness of retinal stimulus electrodes of retinal prostheses in blind subjects.

For future endeavors, biochemical analyses could be attained to detect the different ions concentration as well as the chemical processes of the vitreous. This includes determining the correlation between the temperature, viscosity, liquefaction, oxidation and reduction potentials. This

will enhance our knowledge about this gel-like substance called the vitreous humor.

ACKNOWLEDGEMENTS

We would like to acknowledge the NSF grant FDA SIR: 1445684.

REFERENCES

Bishop, P. N., 2000. *Structural macromolecules and supramolecular organisation of the vitreous gel.* Progress in Retinal and Eye Research, 19, 323-344 ISSN 1350-9462

Krause, C., 1934. *Structural macromolecules and supramolecular organisation of the vitreous gel.* Arch Ophthalmology. 1934;11(6):960-963. doi:10.1001/archopht.1934.00830130044006.

Joseph, N. H., 1990. *Patent US4902292 - Vitreous Body Prosthesis Device*.

Shah, S., Hines, A., Zhou, D., Greenberg, J. R., Humayun, S. M., Weiland, D. J., 2007. *Electrical Properties of Retinal–electrode Interface*. Journal of Neural Engineering.

Kawano, S. I., Honda, Y., and Negi, A., 1982. *Effects of the Biological Stimuli of the Viscosity of the Vitreous*, National Center for Biotechnology Information. U.S. National Library of Medicine.

Clark, D. L., Weiss, A. A., Silver, S., 1977. *Mercury and Organomercurial Resistances Determined by Plasmids in Pseudomonas*. Journal of Bacteriology 132.1 (1977): 186–196. Print.

Loveday D. et al., 2001. *Potentiostatic EIS Tutorial – Getting Started*. https://www.gamry.com/application-notes/EIS/potentiostatic-eis-tutorial/". Web.

Peixoto, N., Jackson, K., Samiyi, R., Minnikanti, S., 2009. *Charge Storage: Stability measures in implantable electrodes*. Engineering in Medicine and Biology Society, 2009. EMBC 2009. Annual International Conference of the IEEE, Minneapolis, MN, 2009, pp. 658-661. doi: 10.1109/IEMBS.2009.5333449

Majdi, J. A., Minnikanti, S., Peixoto, N., Agrawal, A., Cohen, E. D., 2014. *Access resistance of stimulation electrodes as a function of electrode proximity to the retina.* Journal of neural engineering 12, no. 1: 016006.